CHEMISTRY
A EUROPEAN JOURNAL

DOI: 10.1002/chem.200903383

Size Dependence of Nanoscale Confinement on Chiral Transformation

Zhigang Wang,[a, b, c] Chunlei Wang,[a, d] Peng Xiu,[a] Wenpeng Qi,[a] Yusong Tu,[a] Yumei Shen,[a] Ruhong Zhou,[e, f] Ruiqin Zhang,*[b] and Haiping Fang*[a]

Abstract: Molecular dynamic simulations of the chiral transition of a difluorobenzo[*c*]phenanthrene molecule ($C_{18}H_{12}F_2$, D molecule) in single-walled boron-nitride nanotubes (SWBNNTs) revealed remarkable effects of the nanoscale confinement. The critical temperature, above which the chiral transition occurs, increases considerably with the nanotube diameter, and the chiral transition frequency decreases almost exponentially with respect to the reciprocal of temperature. The chiral transitions correlate closely with the orientational transformations of the D molecule. Furthermore, the interaction energy barriers between the D molecule and the nanotube for different orientational states can characterize the chiral transition. This implies that the temperature threshold of a chiral transition can be controlled by a suitable nanotube. These findings provide new insights to the effect of nanoscale confinement on molecular chirality.

Keywords: arenes · chiral transitions · fluorine · molecular dynamics · nanostructures

Introduction

Many of the basic building materials of organisms, such as saccharides and amino acids, are chiral in nature.[1,2] The effect of chirality is very important in molecules used in pharmaceutical products, because the interaction of two chiral molecules strongly depends on their chiralities. There are three different types of chiralities, that is, point, axial, and helical chiralities. The *P*- and *M*-form enantiomers of the difluorobenzo[*c*]phenanthrene molecule ($C_{18}H_{12}F_2$, D molecule) studied in this work belong to the helical chirality. It has long been recognized that some molecules that are chirally stable in bulk systems may display conformational transitions in the human body. For example, in the 1960s, the enantiomeric structure from the chiral transition of thalidomide molecules caused serious damage to fetal growth, known as the "thalidomide tragedy".[3,4] Later, it was found that a chiral transition of thalidomide molecules occurred in human body.[4] Hence, good conformational stability is an important requirement for chiral molecules used in pharmaceutical products.[5] Recently, the conformational transitions of some chiral molecules have been observed experimentally through encapsulation in synthetic cavities.[6–8] In bulk systems, great effort has been invested in this subject for the resolution of chiral molecules.[9–19] The differences in the structure and the spectrum of molecules with different chiralities have been recognized.[20–32] These reports seem to indicate that the confined environment has an active effect on chiral transitions. It is well-known that there are various nanoscale confinement environments in the human body. An understanding of the mechanism of chiral transition is not only useful in the production of chiral pharmaceutical products, but is also helpful in understanding the intricate

[a] Dr. Z. G. Wang, C. L. Wang, P. Xiu, W. P. Qi, Y. S. Tu, Prof. Y. M. Shen, Prof. H. P. Fang
Laboratory of Physical Biology
Shanghai Institute of Applied Physics
Chinese Academy of Sciences
P.O. Box 800-204, Shanghai 201800 (China)
Fax: (+86) 21-59553201
E-mail: fanghaiping@sinap.ac.cn

[b] Dr. Z. G. Wang, Prof. R. Q. Zhang
Center of Super-Diamond and Advanced Films (COSDAF) and
Department of Physics and Materials Science
City University of Hong Kong, Hong Kong SAR (China)
Fax: (+852)-2788-7830
E-mail: aprqz@cityu.edu.hk

[c] Dr. Z. G. Wang
Institute of Atomic and Molecular Physics
Jilin University, Changchun, 130012 (China)

[d] C. L. Wang
Graduate School of the Chinese Academy of Sciences
Beijing 100080 (China)

[e] Prof. R. Zhou
IBM Thomas J. Watson Research Center
Yorktown Heights, NY 10598 (USA)

[f] Prof. R. Zhou
Department of Chemistry, Columbia University
New York, NY 10027 (USA)

differences between bulk systems and confined environment in different research fields.

Confinement of molecules inside nanoscale pores has become an important method of fabricating new structures and exploiting dynamics that do not occur in bulk systems, such as enhanced catalysis,[33–35] and improved stability of the native structure of proteins,[36–38] new mechanisms of protein and polymer dynamics,[39–43] excellent on-off gating, and the ability to control the pumping action of permeation behavior.[44–46] However, the effect of confinement on the conformational transitions is still far from understood.

In this work, we present an approach towards understanding conformational transition by using molecular dynamic (MD) simulations. A series of single-walled boron-nitride nanotubes (SWBNNTs)[47] and a difluorobenzo[*c*]phenanthrene molecule ($C_{18}H_{12}F_2$, D molecule) are used to illustrate the concept. The D molecule has been observed to show the helical chirality transition by using infrared laser pulses.[16] The energy barrier for the chirality transition in bulk was estimated to be only 6.7–8.0 kcal mol^{-1},[16] which indicates that it might be possible to observe this chiral transition in classical MD simulations, particularly with the help of SWBNNT confinements (as shown below the barrier is reduced significantly inside the SWBNNTs). This type of helical chirality transition has also been observed with MD simulations recently for another molecule, 1,2-(1,1-binaphthalene-2,2′-diyldisulfonyl)ethylene, inside a twisted chiral carbon nanotube.[35] Through an aggregate of $\approx$1 μs MD simulations, we observe that the critical temperature, above which the chiral transition occurs, increases with the diameter of the nanotube and the chiral transition frequency decreases almost exponentially with respect to the reciprocal of temperature. The transitions of the D molecule in these nanotubes are mainly controlled by the interaction potential-energy barriers between different conformations of the D molecule that are either parallel or perpendicular to the nanotube axis. These findings are helpful in understanding the transition of chiral molecules and other correlated physical, chemical, and biological processes, which is of particular importance in avoiding chiral transitions related to the safety of some chiral drugs.

Computational Methods

The all-atom-optimized potential for liquid simulations (OPLS-AA) force field was used in our molecular dynamics simulations. The charge population of SWBNNT was calculated using the semi-empirical AM1 method[48] with the Gaussian 03 package.[49] The size of the unit-cell box for all of the systems consisting of a D molecule and a SWBNNT was constructed by the same approach: every directional edge of the SWBNNT was extended to 12 Å. The duration of every simulation was 60 ns, and only the data from the last 50 ns were collected for analysis. The time step used in molecular dynamics simulations was 1 fs, and the data were collected every 0.5 ps. We used position restraint to keep the geometric structure of the SWBNNTs, because our purpose was to study the dynamic behavior of D molecules inside SWBNNTs. All of the dynamic processes were simulated using the Gromacs 3.3.1 program.[50]

The stable geometries of *P* and *M* chiral enantiomers of D molecules were situated in one of the symmetric double potential wells.[16] The chiral character of different enantiomers can be characterized by dihedral angle of four atoms (a-b-c-d) shown in Figure 1 (top). When the dihedral angle is averaged over a certain time period (here, we use 0.1 ns), the value of the chiral character is positive if the form belongs to a *P* enantiomer and negative if it is an *M* enantiomer.

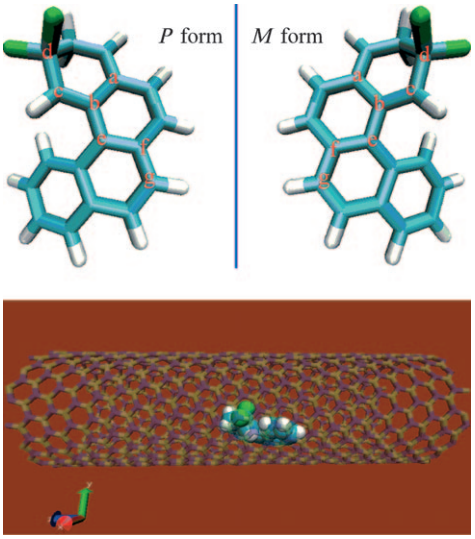

Figure 1. Top: *P*- and *M*-form enantiomers of a D molecule. The letters a, b, c, and d denote the corresponding atoms of two enantiomers, which are used to identify the chiral geometry of the different enantiomers. These atoms marked by e, f and g are used to determine a plane of the D molecule. Bottom: the D molecule inside a (15,6) SWBNNT.

We used the (13,4), (14,5), (15,6), (16,7), and (17,8) SWBNNTs with diameters ranging from 12.0 to 17.3 Å. The lengths of these SWBNNTs are about 40 Å. From the semi-empirical quantum mechanics AM1 method, the boron atoms carry charges of about 0.30 e and nitrogen atoms carry charges of −0.30 e. Our current simulations showed that the conclusions are insensitive to the exact values of these charges and numerical results do not change much when boron atom charges are within 0.05 e (fluctuation) from 0.30 e. For simplicity, and without loss of generality, in our simulations a charge of 0.30 e was attached to each boron atom and a charge of −0.30 e was attached to each nitrogen atom. Our classical molecular dynamic simulations were performed on the system of chiral enantiomers inside the SWBNNTs at different temperatures (see Figure 1, bottom).

Results and Discussion

Figure 2 a and b show the chiral character of *P*- and *M*-form enantiomers inside a (15, 6) SWBNNT at 420 K. It is clear that in all of the 50 ns simulations, the averaged values of the dihedral angle (for each 0.1 ns) for each nanosecond interval keep their original signs, indicating that both the *P*- and *M*-form enantiomers are stable below 420 K. The transition between the structures of chiral enantiomers is observed at 440 K and above as shown in Figure 2 c and d. A typical structural trajectory of the D molecule showing the helical chirality transition at 440 K is displayed in Figure 3. Similar observations are also made in the other SWBNNTs

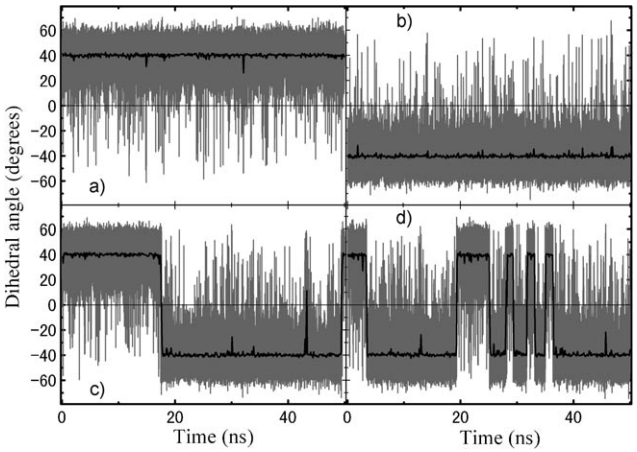

Figure 2. Dihedral angle of the D molecule as a function of time (gray curve) in a (15, 6) SWBNNT at different temperatures. a) An initial *P* form at 420 K. b) An initial *M* form at 420 K. c) An initial *P* form at 440 K showing chiral transitions. d) An initial *P* form at 460 K showing chiral transitions. The value is positive for *P*- and negative for *M*-form enantiomers. The averaged values for each 0.1 ns are indicated with the black curves.

in which the transition occurs at different temperature thresholds. We have computed the critical temperature T_C for the transitions of enantiomers inside different SWBNNTs. In our study, the critical temperature (or temperature threshold) T_C is defined as the temperature at which the enantiomers of D molecules can transform within 30 ns, while the enantiomer is kept intact at T_C −20 K for 30 ns for a large number of trajectories starting from different initial configurations. By this definition, the error bars of T_C are approximately 20 K.

The result in Figure 4 (top) shows that T_C increases monotonically as the diameter of the SWBNNT increases. We also calculated the chiral transition frequencies for different temperatures in (15,6), (14,5), and (13,4) SWBNNTs, and the results are shown in Figure 4 (bottom). It is interesting to find that they can be fitted with the Arrhenius activation energy function (i.e., $f=f_0\exp(-E_a/k_BT)$) very well, in which f is the chiral transition frequency, E_a is the activation energy, and k_B is the Boltzmann constant. Here $f_0=937$, 139, 276 ns^{-1} and $E_a=36$, 18, 17 $kJ\,mol^{-1}$ for (15,6), (14,5), and (13,4) SWBNNTs, respectively.

Now we focus on how enantiomer transitions occur in our nanotubes and the mechanism behind those numerical observations. The D molecule consists of four six-membered rings, and has a close to a planar structure. At low temperatures, the D molecule usually clings to the inside surface of the SWBNNT, that is, its surface parallel to the SWBNNT axis, as shown in Figure 5a.

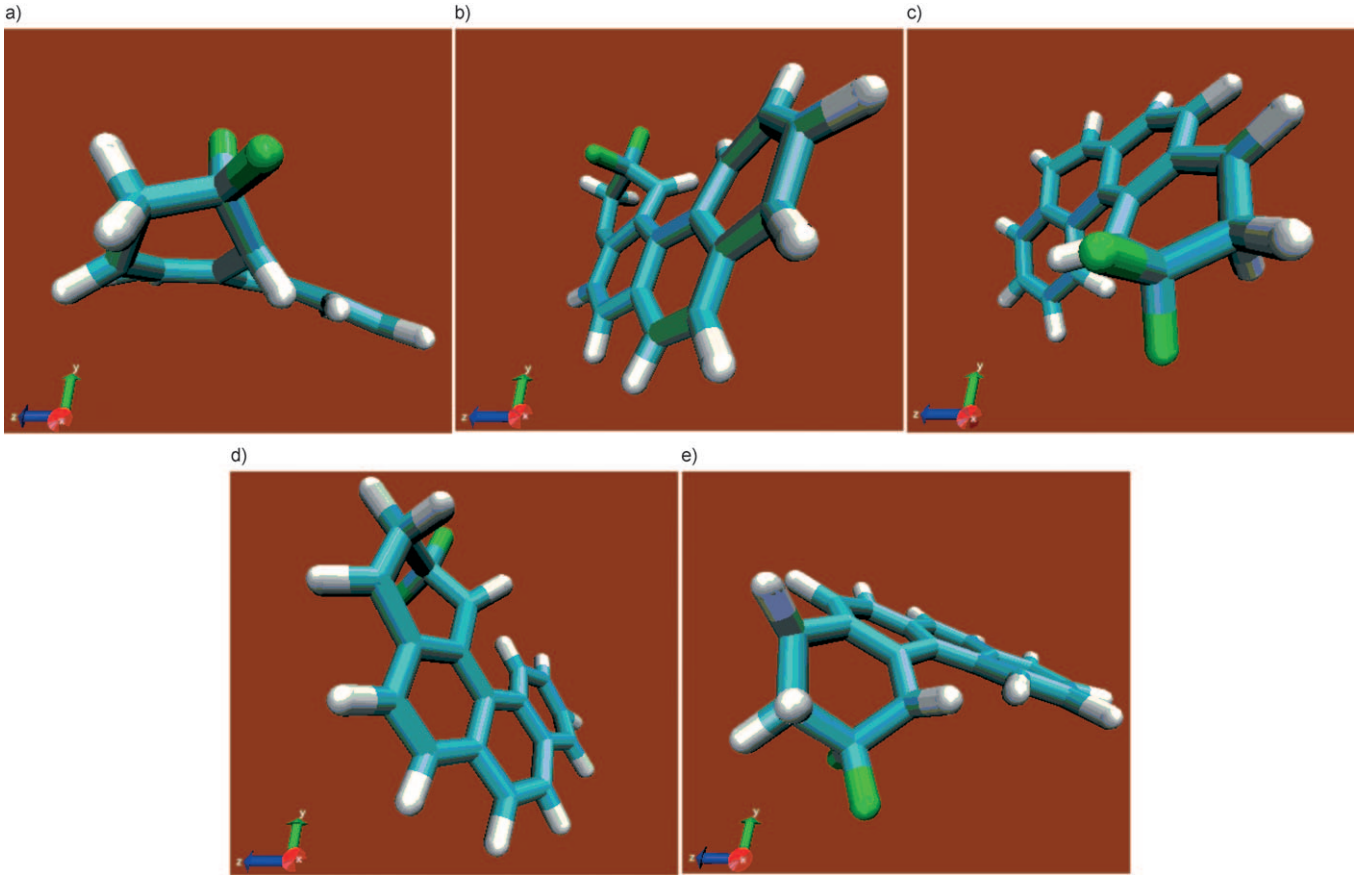

Figure 3. A structural trajectory of the D molecule showing the transition from the *P* to the *M* form as described in Figure 2c. a) $t=17.4515$ ns. b) $t=17.504$ ns. c) $t=17.5565$ ns. d) $t=17.609$ ns. e) $t=17.6615$ ns.

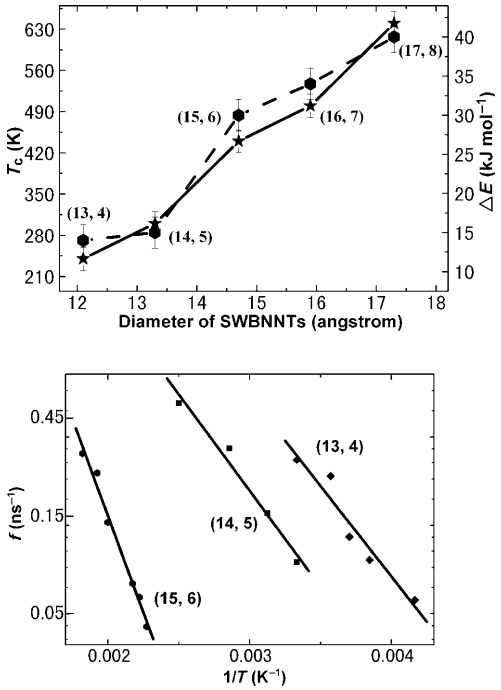

Figure 4. Top: Critical transition temperature T_C (star representation, corresponding to the left axis) and the corresponding interaction energy barrier ΔE between the SWBNNT and the D molecules in the chiral transition process (dashed line, corresponding to the right axis). Bottom: The dependence of the chiral transition frequency (f) on temperature (T). The solid lines are the fits for the exponential functions $f=f_0\exp(-E_a/k_BT)$ for different SWBNNTs; see text for values of f_0 and E_a.

We found that, in each successful transition, the D molecule first changes its orientation so that the angle between the D molecule and the axes of the SWBNNTs increases considerably; it even reaches 90° in a nanotube with a large diameter, such as a (15,6) SWBNNT, as shown in the example in Figure 5b. This is quite different from the chiral transition in bulk systems. Here the angle between the D molecule and the axis of SWBNNTs is defined as the angle between the plane determined by atoms e, f, and g (see Figure 1 top for labeling system) of the D molecule and the axis of SWBNNTs. When the D molecule clings to the nanotube again (see Figure 5c), its chirality may be changed. We computed the interaction potential energy between the SWBNNT and the D molecule, which includes both the van der Waals interactions and the Coulomb interactions. The interaction energy for a transition inside a (15,6) SWBNNT is shown in Figure 5d. It is clear that the interaction energy for a D molecule that clings to the inside surface is lower (at about 30 kJ mol^{-1}) than the energy for a D molecule that

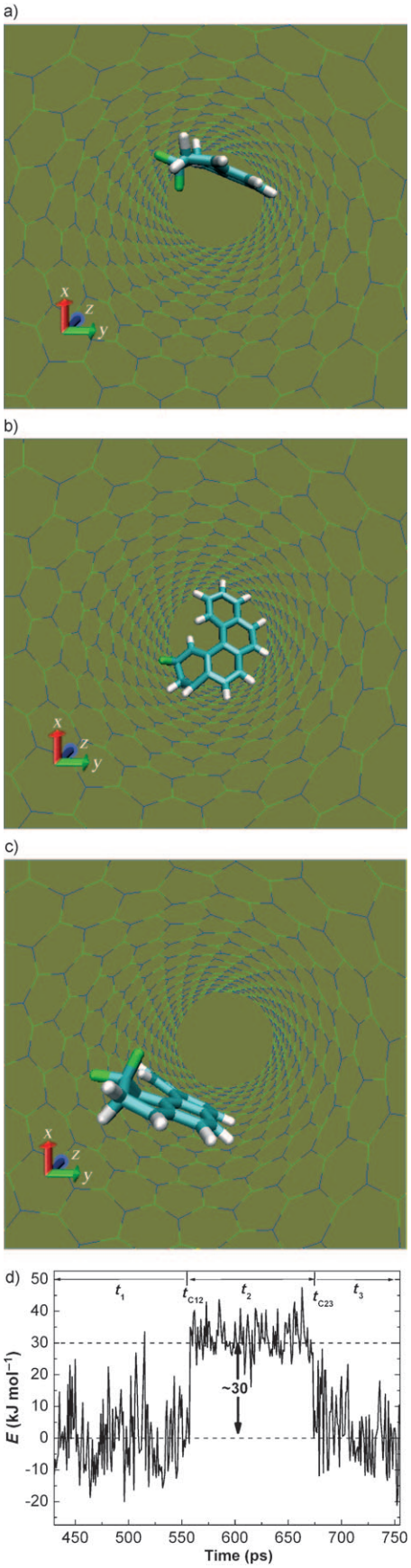

Figure 5. Typical configurations of the D molecule transformed from one chiral form to another inside a (15, 6) SWBNNT (a–d) together with the interaction potential E for a transition. a)–c) represent typical geometries in time periods t_1, t_2, and t_3, respectively. These typical geometries are indicated by t_1, t_2, and t_3 in d). All energies are relative to the average value of time periods t_1 and t_3.

is almost perpendicular to the nanotube axis. Careful examination shows that the difference in the interaction potential energy is almost completely due to the van der Waals interactions between the SWBNNT and the D molecule; the Coulomb interactions between the SWBNNT and the D molecule are very small (in the order of 0.1 kJ mol^{-1}).

To further characterize the difference of the chiral transition in confined environments and bulk systems, we have computed the free energy of the chiral transition of the D molecule at the room temperature (300 K). The results for the (13,4) and (14,5) SWBNNTs are shown in Figure 6. The

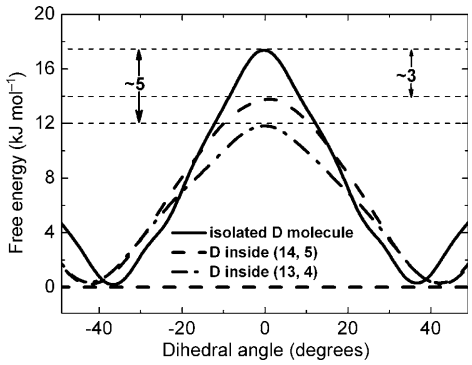

Figure 6. Free energy of the D molecule when changing from one chiral form to another inside the (13,4) and (14,5) SWBNNTs and in the bulk system (isolated D molecule). The minimum point of the free energy is chosen as the reference zero point for each curve.

free energy of the chiral transition of the D molecule in an SWBNNT is defined as $F=-k_BT\ln(S_\alpha)$, in which S_α is the probability of the appearance of the dihedral angle (a-b-c-d) α. For the calculation of the free energy of the D molecule in the bulk system, umbrella sampling[51] with a weighted histogram analysis method (WHAM)[52] was employed. The dihedral angles (a-b-c-d) were restrained to values $\alpha=-48+n\times 8$ ($n=0$, 1, 2 ...12), and the force constant of restraint is 400 kJ mol^{-1} rad^{-2}. The result indicates that the barrier height of the free energy for the chiral transition inside the SWBNNTs is considerably lower (e.g., about 5 kJ mol^{-1} lower inside the (13, 4) SWBNNT) than that of the bulk system.

We also calculated the interaction potential energy barrier ΔE for the chiral transitions in different SWBNNTs. The results are co-plotted in Figure 4 (top, dashed line, right-hand axis). The interaction energy barrier is defined as the averaged value of the interaction potential energy in the t_2 period, minus the average value in the t_1 and t_3 periods, as shown in Figure 5d. In our computation, the start and end points of the t_2 period are defined from the geometric trajectories of the D molecule. The starting point, denoted by t_{C12}, is defined as the point at which the angle between the D molecule and the axes of the SWBNNT θ, averaged over 2 ps, is less than 45° before t_{C12}, and larger than 45° after t_{C12}. Similarly, before the end point of period t_2, denoted by t_{C23}, the averaged value of θ for the first 2 ps is not less than 45°, and the averaged value of θ after t_{C23} is less than 45°. These definitions were based on the fact that the change of angle θ from about 0° to above 45° around t_{C12} (or from above 45° to 0° around t_{C23}) always occurred within 2 ps in our simulations. For each SWBNNT, we obtained five chiral transitions from numerical simulations. Each point of the potential barrier ΔE shown in Figure 4 (top) is the average value of those five transitions. In addition, we computed the error bars, which are about 2 kJ mol^{-1}, and found them to be much smaller than the potential barriers. The interaction potential-energy barrier gradually increases with the diameter of the SWBNNTs. Remarkably, the behavior of the increase of the potential barrier ΔE with respect to the diameter of the nanotube is quite similar to the behaviour of the threshold temperature T_C. Thus, it seems that the transition temperature T_C for the D molecule is mainly determined by the transition barrier from a conformation parallel to the nanotube axis to a conformation perpendicular to the nanotube axis. Therefore, we can control transition temperature by using SWBNNTs with different diameters.

Since the chiral transitions correlate closely with orientational transformations, which are characterized by the energy barrier of the interactions between the D molecule and the nanotube for different orientational states, we expect that as the temperature increases, which enhances the thermal fluctuations, the chiral transition happens more frequently. This further demonstrates that the chiral transitions may be governed by the potential barriers of the orientational transformations.

Conclusion

In summary, nanoscale confinement has an active effect on chiral transition. It is shown that the transition usually occurs under orientation transformation of the molecules from a state parallel to the nanotube axis to a state almost perpendicular to the nanotube axis. Furthermore, the interactions between the chiral molecule and the nanochannel (mainly the van der Waals interactions) can characterize the chiral transition between these two conformation states. This observation implies that the threshold of the chiral transition temperature can be controlled by using suitable nanotubes.

Acknowledgements

The work was supported by the Research Grants Council of Hong Kong SAR (project No. CityU 103907), the National Science Foundation of China (under grant No. 10825520), the National Basic Research Program of China (under grant No. 2007CB936000), the Knowledge Innovation Program of Shanghai Institute of Applied Physics of the Chinese Academy of Sciences, and Shanghai Supercomputer Center of China. Z.G.W. acknowledges the support of K. C. Wong Education Foundation, Hong Kong, China, and Special Fund for Basic Research in National Universities. R.Z. acknowledges the support from the IBM BlueGene Science Program.

[1] R. A. Sheldon, *Chirotechnology*, Dekker, New York, **1993**.
[2] D. B. Cline, *Physical Origin of Homochirality in Life*, AIP, Woodbury, **1996**.
[3] G. Blaschke, H. P. Kraft, H. Markgraf, *Chem. Ber.* **1980**, *113*, 2318.
[4] T. Eriksson, S. Björkman, B. Roth, A. Fyge, P. Höglund, *Chirality* **1998**, *10*, 223.
[5] J. Caldwell, *Chem. Ind.* **1995**, *5*, 176.
[6] M. Inouye, M. Waki, H. Abe, *J. Am. Chem. Soc.* **2004**, *126*, 2022.
[7] M. Waki, H. Abe, M. Inouye, *Angew. Chem.* **2007**, *119*, 3119; *Angew. Chem. Int. Ed.* **2007**, *46*, 3059.
[8] H. Abe, H. Machiguchi, S. Matsumoto, M. Inouye, *J. Org. Chem.* **2008**, *73*, 4650.
[9] S. H. Wilen, J. Z. Qi, P. G. Williard, *J. Org. Chem.* **1991**, *56*, 485.
[10] J. F. Larrow, E. N. Jacobsen, Y. Gao, Y. P. Hong, X. Y. Nie, C. M. Zepp, *J. Org. Chem.* **1994**, *59*, 1939.
[11] P. J. Harrington, E. Lodewijk, *Org. Process Res. Dev.* **1997**, *1*, 72.
[12] M. Periasamy, *Aldrichimica Acta* **2002**, *35*, 89.
[13] T. Brotin, R. Barbe, M. Darzac, J.-P. Dutasta, *Chem. Eur. J.* **2003**, *9*, 5784.
[14] J. Schindler, M. Egressy, J. Bálint, Z. Hell, E. Fogassy, *Chirality* **2005**, *17*, 565.
[15] K. Sakai, R. Sakurai, N. Hirayama, *Top. Curr. Chem.* **2006**, *269*, 233.
[16] H. Umeda, M. Takagi, S. Yamada, S. Koseki, Y. Fujimura, *J. Am. Chem. Soc.* **2002**, *124*, 9265.
[17] N. P. M. Huck, W. F. Jager, B. de Lange, B. L. Feringa, *Science* **1996**, *273*, 1686.
[18] T. Vries, H. Wynberg, E. van Echten, J. Koek, W. ten Hoeve, R. M. Kellogg, Q. B. Broxterman, A. Minnaard, B. Kaptein, S. van der Sluis, L. Hulshof, J. Kooistra, *Angew. Chem.* **1998**, *110*, 2491; *Angew. Chem. Int. Ed.* **1998**, *37*, 2349.
[19] "Optical Resolution by Inclusion Complexation with a Chiral Host Compound": *Enantiomer Separation: Fundamentals and Practical Methods* (Ed.: F. Toda), Kluwer Academic, New York, **2004**.
[20] B. L. Feringa, R. A. van Delden, N. Koumura, E. M. Geertsema, *Chem. Rev.* **2000**, *100*, 1789.
[21] G. A. Hembury, V. V. Borovkov, Y. Inoue, *Chem. Rev.* **2008**, *108*, 1.
[22] M. S. Strano, *J. Am. Chem. Soc.* **2003**, *125*, 16148.
[23] G. Dukovic, M. Balaz, P. Doak, N. D. Berova, M. Zheng, R. S. McLean, L. E. Brus, *J. Am. Chem. Soc.* **2006**, *128*, 9004.
[24] X. Peng, N. Komatsu, S. Bhattacharya, T. Shimawaki, S. Aonuma, T. Kimura, A. Osuka, *Nat. Nanotechnol.* **2007**, *2*, 361.
[25] Q. Chenand, N. V. Richardson, *Nat. Mater.* **2003**, *2*, 324.
[26] A. Kühnle, T. R. Linderoth, B. Hammer, F. Besenbacher, *Nature* **2002**, *415*, 891.
[27] J. A. Switzer, H. M. Kothari, P. Poizot, S. Nakanishi, E. W. Bohannan, *Nature* **2003**, *425*, 490.
[28] C. A. Orme, A. Noy, A. Wierzbicki, M. T. McBride, M. Grantham, H. H. Teng, P. M. Dove, J. J. DeYoreo, *Nature* **2001**, *411*, 775.
[29] J. W. Kim, M. Carbone, J. H. Dil, M. Tallarida, R. Flammini, M. P. Casaletto, K. Horn, M. N. Piancastelli, *Phys. Rev. Lett.* **2005**, *95*, 107601.
[30] S. Blankenburg, W. G. Schmidt, *Phys. Rev. Lett.* **2007**, *99*, 196107.
[31] R. B. Rankin, D. S. Sholl, *J. Chem. Phys.* **2006**, *124*, 074703.
[32] C. Girardet, D. Vardanega, F. Picaud, *Chem. Phys. Lett.* **2007**, *443*, 113.
[33] X. L. Pan, Z. L. Fan, W. Chen, Y. J. Ding, H. Y. Luo, X. H. Bao, *Nat. Mater.* **2007**, *6*, 507.
[34] H. Q. Yang, L. Zhang, L. Zhong, Q. H. Yang, C. Li, *Angew. Chem.* **2007**, *119*, 6985; *Angew. Chem. Int. Ed.* **2007**, *46*, 6861.
[35] B. Y. Wang, P. Kra, I. Thanopulos, *Nano Lett.* **2006**, *6*, 1918.
[36] D. K. Eggers, J. S. Valentine, *Protein Sci.* **2001**, *10*, 250.
[37] D. Lucent, V. Vishal, V. S. Pande, *Proc. Natl. Acad. Sci. USA* **2007**, *104*, 10430.
[38] W. X. Xu, J. Wang, W. Wang, *Proteins* **2005**, *61*, 777.
[39] H. J. Gao, Y. Kong, D. X. Cui, C. S. Ozkan, *Nano Lett.* **2003**, *3*, 471.
[40] R. H. Zhou, X. H. Huang, C. J. Margulis, B. J. Berne, *Science* **2004**, *305*, 1605.
[41] S. Q. Zhang, M. S. Cheung, *Nano Lett.* **2007**, *7*, 3438.
[42] A. Cacciuto, E. Luijten, *Nano Lett.* **2006**, *6*, 901.
[43] C. Y. Bao, Q. Gan, B. Kauffmann, H. Jiang, I. Huc, *Chem. Eur. J.* **2009**, *15*, 11530.
[44] R. Z. Wan, J. Y. Li, H. J. Lu, H. P. Fang, *J. Am. Chem. Soc.* **2005**, *127*, 7166.
[45] J. Y. Li, X. J. Gong, H. J. Lu, D. Li, H. P. Fang, R. H. Zhou, *Proc. Natl. Acad. Sci. USA* **2007**, *104*, 3687.
[46] X. J. Gong, J. Y. Li, H. J. Lu, R. Z. Wan, J. C. Li, J. Hu, H. P. Fang, *Nat. Nanotechnol.* **2007**, *2*, 709.
[47] D. Golberg, Y. Bando, C. C. Tang, C. Y. Zhi, *Adv. Mater.* **2007**, *19*, 2413.
[48] M. J. S. Dewar, E. G. Zoebisch, E. F. Healy, *J. Am. Chem. Soc.* **1985**, *107*, 3902.
[49] Gaussian 03, Revision D.01, M. J. Frisch, G. W. Trucks, H. B. Schlegel,G. E. Scuseria, M. A. Robb, J. R. Cheeseman, J. A. Montgomery, Jr., T. Vreven, K. N. Kudin, J. C. Burant, J. M. Millam, S. S. Iyengar, J. Tomasi, V. Barone, B. Mennucci, M. Cossi, G. Scalmani, N. Rega, G. A. Petersson, H. Nakatsuji, M. Hada, M. Ehara, K. Toyota, R. Fukuda, J. Hasegawa, M. Ishida, T. Nakajima, C. Adamo, J. Maramillo, R. Gomperts, R. E. Stratmann, O. Yazyev, A. J. Austin, R. Cammi, C. Pomelli, J. W. Ochterski, P. Y. Ayala, K. Morokuma, G. A. Voth, P. Salvador, J. J. Dannenberg, V. G. Zakrewski, S. Dapprich, A. D. Daniels, M. C. Strain, O. Farkas, D. K. Malick, A. D. Rabuck, K. Raghavachari, J. B. Foresman, J. V. Ortiz, Q. Cui,A. G. Baboul, S. Clifford, J. Cioslowski, B. B. Stefanov, G. Liu, A. Liashenko, P. Piskorz, I. Komaromi, R. L. Martin, D. J. Fox, T. Keith, M. A. Al-Laham, C. Y. Peng, A. Nanayakkara, M. Challacombe, P. M. W. Gill, B. Johnson, W. Chen, M. W. Wong, C. Gonzalez, J. A. Pole, Gaussian Inc., Wallingford CT, **2004**.
[50] D. van der Spoel, E. Lindahl, B. Hess, G. Groenhof, A. E. Mark, H. J. C. Berendsen, *J. Comput. Chem.* **2005**, *26*, 1701.
[51] "A Guide to Monte Carlo for Statistical Mechanics: 2. Byways": J. P. Valleau, G. M. Torrie in *Statistical Mechanics. Part A: Equilibrium Techniques, Vol. 5* (Ed.: B. J. Berne), Plenum, New York, **1977**.
[52] S. Kumar, D. Bouzida, R. H. Swendsen, P. A. Kollman, J. M. Rosenberg, *J. Comput. Chem.* **1992**, *13*, 1011.

Received: December 10, 2009
Revised: April 4, 2010
Published online: May 18, 2010

